ISSN(Online) : 2319-8753
ISSN (Print) : 2347-6710

International Journal of Innovative Research in Science, Engineering and Technology

(An ISO 3297: 2007 Certified Organization)

Website: www.ijirset.com

Vol. 6, Issue 1, January 2017

DC Conductivity Study of Ferrofluid of Fe_3O_4 Ferrite Nanoparticles Dispersed in Hydrocarbon Carrier

S. D. Kemkar[1], Milind Vaidya[2], Deepak Pinjari[3], Anand Jadhav[4], Sanjana Kemkar[5], Siddhesh Nanaware[6], Sanjukta Kemkar[7]

PhD Student, Department of Physics, Smt. Chandibai Himathmal Mansukhani College, Ulhasnagar, India[1]

Principal, Department of Physics, Vedanta College , Vithalwadi, India[2]

Assistant Professor, Department of Chemical Engineering, Institute of Chemical Technology, Mumbai, India[3]

PhD Student, Department of Chemical Engineering, Institute of Chemical Technology, Mumbai, India[4]

Student, Smolensk State Medical University, Smolensk, Russia[5]

B.E Graduated, Department of Mechanical Engineering, STES NBN Sinhgad School of Engineering, Pune, India[6]

Student, Department of Microbiology, Smt. Chandibai Himathmal Mansukhani College, Ulhasnagar, India[7]

ABSTRACT: This work describes the preparation of suspensions consisting of hydrophobic magnetite nanoparticles dispersed in kerosene. The ferrite particles are covered by a shell of chemisorbed oleate ions. The resulting oleate-covered particles were analysed by FTIR, XRD, conductivity and TEM studies. In the present work, use of ferrofluid in fabrication of fixed as well as variable resistive component of electrical network for industrial application has been investigated. Test cells with different inter-electrode spacing were also fabricated for studying the effect of electric field on conductivity in turn resistivity of ferrofluid.

KEYWORDS: DC conductivity, Fe_3O_4 nanoparticle, Ferrofluid, particle size, XRD.

I. INTRODUCTION

Ferrofluid is a dispersion of ferrimagnetic nanoparticles in either polar or non-polar liquid carriers. Different methods have been used to prepare magnetic nanoparticles, including wet grinding, co-precipitation of metal salts in aqueous solution, micro emulsion techniques, the decomposition of organometallic compounds and the reduction of metal salts. Dispersion of ferrimagnetic nanoparticles in non-polar liquid carriers results into particle aggregation and hence large rate of sedimentation of the aggregates due to van der Waals attraction. Coating of the particles with long-chain molecules containing a polar group and a tail with dielectric properties similar to the carrier liquid reduces its sedimentation of ferrimaganetic nanoparticles in polar liquid carrier. Ferrofluids are widely studied for their applications in various fields in biology and medicine such as enzyme and protein immobilization, genes, radiopharmaceuticals, magnetic resonance imaging (MRI) [1], diagnostics, immunoassays, purification, separation, and controlled drug release [2-4]. Ferrofluids characteristically have both, magnetic and fluidic properties and have found a diverse range of applications in electrical engineering [5,6] as well as specific applications like sensors [7,8], optical fibres [9,10]in audio devices [11], inertia dampers, stepper motors [12], vacuum seals[13,14], electromagnetic shielding [15], microwave [16,17] and high density digital storage.

In the present work, the synthesis of oleate-coated ferrimagnetic nanoparticles has been reported and its DC conductivity study has been carried out for the purpose of optimising use of ferrofluid in similar applications like Voltage Dependant

ISSN(Online) : 2319-8753
ISSN (Print) : 2347-6710

International Journal of Innovative Research in Science, Engineering and Technology

(An ISO 3297: 2007 Certified Organization)

Website: www.ijirset.com

Vol. 6, Issue 1, January 2017

Resistor (VDR). Kerosene as carrier liquid was used to determine its adequate coupling with the hydrocarbon tail of coating material leading to stable ferrofluids. Finally, the oleate-coated magnetite powder and the ferrofluid suspensions were tested in 3 test cells.

In liquid, there are two types of conduction of electricity, i.e. ionic and electronic or both. In solids, generally only electronic conduction takes place. Electronic conduction in conducting polymer is due to hopping of electrons [18, 19]. In this work, the conductivity is mainly due to ions.

II. SYNTHESIS OF Fe_3O_4 NANOPARTICLE

1. Materials

Materials used for preparation of nano particles were $FeCl_3$:$6H_2O$ with 97 % purity, $FeCl_2$:$4H_2O$ with 99 % of purity [20] and high grade NaOH. Oleic acid ($C_{18}H_{34}$ O_2) was used as a surfactant for steric stabilisation of particle. Milli-Q water was re-deionized with specific conductance < 0.1 S/cm and deoxygenated by bubbling with N_2 gas for 1hr prior to use.

Kerosene was used as a non polar hydrocarbon carrier liquid. Particles were prepared by chemical co precipitation method and then suspended in carrier liquid. Then the particles were stabilized by Oleic acid as a surfactant. Three batches of particles were prepared by changing environment during reaction like preparation time, rate of flow of ionic solution in basic, pH of the solution, reaction temperature, molar concentration etc.

2. Procedure for preparation of nano particles

Ferrimagnetic nanoparticles were prepared by co-precipitation method by taking salts with 1.28M $FeCl_3$. $6H_2O$ and 0.64M $FeCl_2$. $4H_2O$ was mixed vigorously. 1.5M NH_4OH was added to the Fe^{2+}/Fe^{3+} ionic solution under vigorous mechanical stirring. The principle reaction is shown in equation -1.

$$2Fe^{3+} + Fe^{2+} + 4OH^- \longrightarrow Fe_3O_4 + 4\,H^+ \qquad (1)$$

0.5 ml of 1M hydrochloric acid (HCL) was used in order to neutralize the anionic charge on the surface of the nanoparticles. Various batches were prepared under different pH (8, 10 and 12). 8 ml of oleic acid was added to the alkaline solution and the resulting emulsion was kept under vigorous mechanical stirring at room temperature for 1 hr. Precipitate was put in the solution and heated up to 95 ^{0}C for surfactant treatment. When the desired temperature was obtained, the suspension was allowed to cool down to room temperature while surface anionic charge was neutralised. At pH of 4.5 to 5, chemisorptions of oleate ions have taken place on nano particles. Thereafter the coagulation and settling down of coagulation in the solution has taken place this was due to the fact that the hydrophobicity provided by the tails in oleate layer. The precipitate was washed three times with acetone in order to remove any impurities as well as excessive surfactant from the solution. Later on precipitate was washed four times with deionised distilled water. Collected particles were turned from dark black to brownish shade on surfactant treatment. These particles were dispersed in kerosene for making ferrofluid. Ferrofluid was centrifuged for 1 hr at 3500 rpm and lump was removed.

3. Preparation of ferrofluid samples.

Nanoparticle sample made at pH 8 were dispersed in kerosene with volume concentrations of 0.25%, 0.5%, 1%, 2% were prepared as ferrofluid samples. All these 4 ferrofluid samples are grouped together as S_pH8. This was repeated for pH10 and pH12 and the samples were grouped as S_pH10 and S_pH12 respectively. In this way, a total 12 numbers of ferrofluid samples were prepared.

III. CHARACTERIZATION OF Fe_3O_4 NANOPARTICLES

Three batches of nanoparticles were prepared at S_pH8, S_pH10 and S_pH12. XRD, TEM, VSM and FTIR characterizations were carried out on these samples. Fig 1. – Fig 3. shows characterization of XRD performed on X-ray diffractometer Phillips PW 1800, range 6-80^o.

ISSN(Online) : 2319-8753
ISSN (Print) : 2347-6710

International Journal of Innovative Research in Science, Engineering and Technology

(An ISO 3297: 2007 Certified Organization)

Website: www.ijirset.com

Vol. 6, Issue 1, January 2017

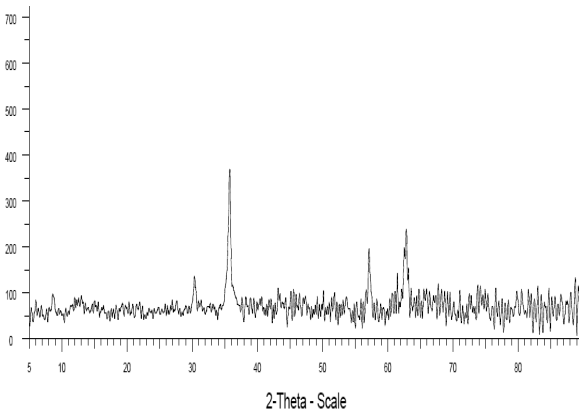

Fig. 1: XRD Pattern of Fe_3O_4 nanoparticle of size 29.6nm
x-axis: 2 Theta y-axis: Intensity a.u.

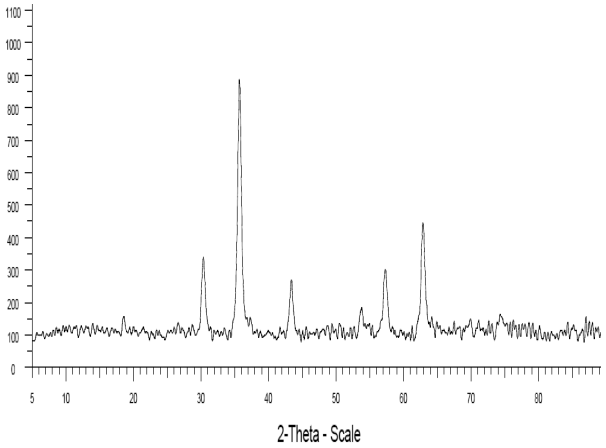

Fig. 2: XRD Pattern of Fe_3O_4 nanoparticle of size18.7nm
x-axis: 2 Theta y-axis: Intensity a.u.

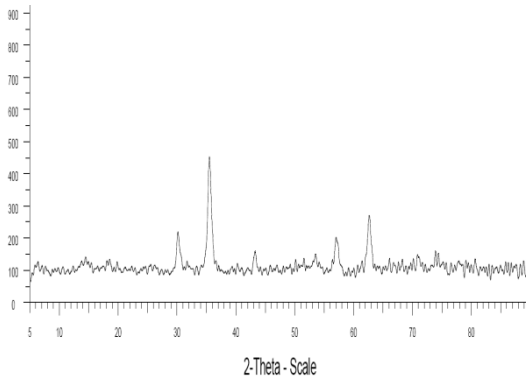

Fig. 3: XRD Pattern of Fe_3O_4 nanoparticle of size 9.2nm
x-axis: 2 Theta y-axis: Intensity a.u.

The particle sizes of these nanoparticles were characterized by Transmission Electron Microscopy, TEM, H-7650 with accelerating voltage of 200 KV as shown from Fig 4 - Fig 6.

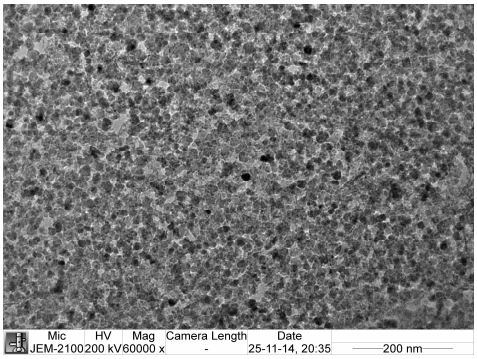

Fig. 4: TEM image of Fe_3O_4 ferrofluid sample of average size 30nm

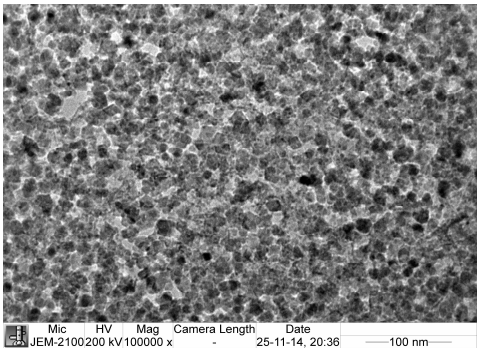

Fig. 5: TEM image of Fe_3O_4 ferrofluid sample of average size 19nm

ISSN(Online) : 2319-8753
ISSN (Print) : 2347-6710

International Journal of Innovative Research in Science, Engineering and Technology

(An ISO 3297: 2007 Certified Organization)

Website: www.ijirset.com

Vol. 6, Issue 1, January 2017

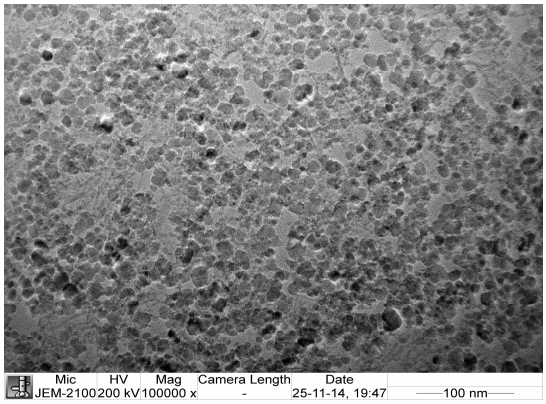

Table no. 1

D_{TEM}	10nm	19nm	30nm
D_{XRD}	9.2nm	18.7nm	29.6nm
M_{sat}	63.5emu/cc	76.0emu/cc	82.21emu/cc

Fig. 6: TEM image of Fe_3O_4 ferrofluid sample of average size 10nm

Magnetic characterization of the nanoparticles was carried using Vibrating Sample Magnetometer (VSM) shown in Fig-7, with a magnetic field in the range of ± 1 Tesla at 300K, as the application was intended to be used in room temperature. The behaviour of nanofluids is mainly determined by their magnetic properties.

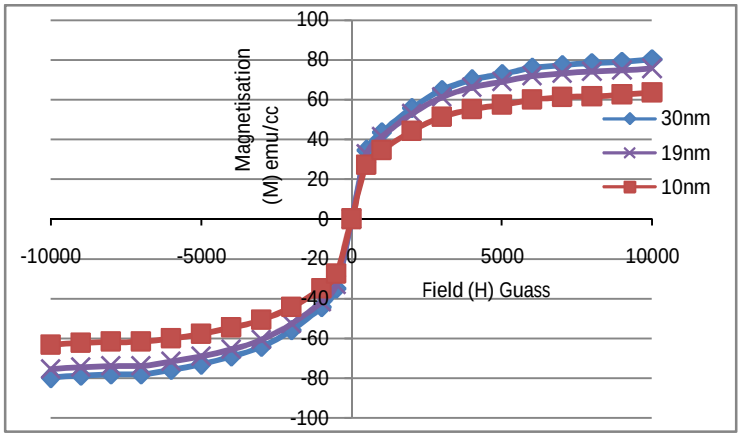

Fig. 7: Magentisation (M) vs Field (H) for Fe_3O_4@300K

FTIR was carried out on all three samples to investigate the absorption of oleic acid molecules as per Fig.8 – Fig.10. This can be investigated on the basis of signature of double bond seen at around 1710 cm^{-1}.

ISSN(Online) : 2319-8753
ISSN (Print) : 2347-6710

International Journal of Innovative Research in Science, Engineering and Technology

(An ISO 3297: 2007 Certified Organization)

Website: www.ijirset.com

Vol. 6, Issue 1, January 2017

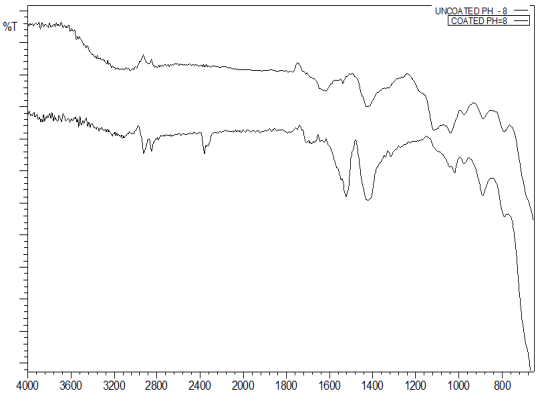

Fig. 8: X-axis: cm^{-1}, Y-axis: Transmittance

[FTIR of Fe_3O_4 nanoparticles of size 30nm (pH=8) with and without coating. Absorbance around 1710 cm^{-1} is indication of C=O bonding. Shows evidence of oleic acid adsorbtion on nanoparticles.]

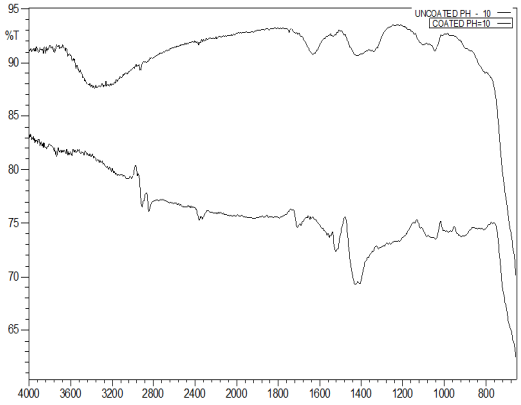

Fig. 9: X-axis: cm^{-1}, Y-axis: Transmittance

[FTIR of Fe_3O_4 nanoparticles of size 19nm (pH=10) with and without coating. Absorbance around 1710 cm^{-1} is indication of C=O bonding. Shows evidence of oleic acid adsorbtion on nanoparticles.]

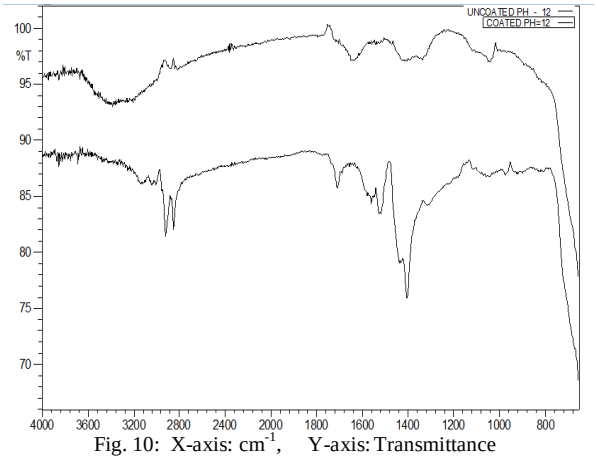

Fig. 10: X-axis: cm^{-1}, Y-axis: Transmittance

[FTIR of Fe_3O_4 nanoparticles of size 10nm (pH=12) with and without coating. Absorbance at 1710 cm^{-1} is indication of C=O bonding Shows evidence of oleic acid adsorbtion on nanoparticles.]

IV. EXPERIMENTAL SET UP FOR CONDUCTIVITY MEASUREMENT

Variable Voltage source consists of multitap AC transformer (rating 20Volts AC to Multiple Output voltages). These were further converted to DC by bridge rectifier circuit and regulated. Output smoothening capacitors were employed to get DC voltage with minimum ripple. Inter-electrode potential was varied as 0V to 35V with 5V intervals. DC Output was measured across R_L-C smoothening parallel network of resistance 100K and 0.01µF capacitance connected to the cell. A capacitor was used to reduce electrical noise. R_L-C network was connected in series with cell D1, D2 and D3. FET high input impedance electronic voltmeter was used to measure V_{out} at R_L-C network. FET high input impedance voltmeter was used to reduce loading effect of voltmeter on output voltage of the cells. This setup is an

ISSN(Online) : 2319-8753
ISSN (Print) : 2347-6710

International Journal of Innovative Research in Science, Engineering and Technology

(An ISO 3297: 2007 Certified Organization)

Website: www.ijirset.com

Vol. 6, Issue 1, January 2017

alternative method for measuring DC conductivity.

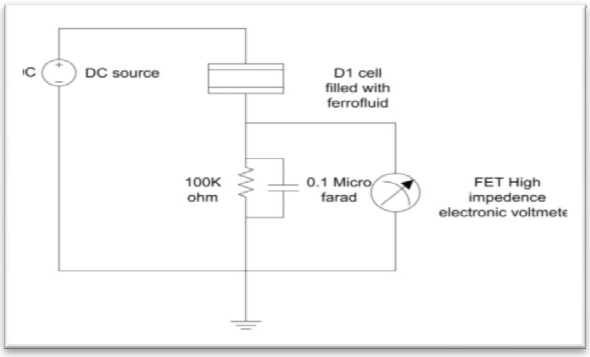

Fig. 11: Electrical Network for the application of ferrofluid in fixed resistive components

Three test cells were used viz D1, D2, D3 having inter-electrode spacing of 3mm, 6mm and 9mm respectively. Electrodes used in these test cells were circular copper plates having diameter of 26 mm. Appropriate contacts were drawn from the electrodes for further connections. Particle sample S_pH8 was used in different ferrofluids with concentrations 0.25%, 0.5%, 1% and 2% were used. Each concentration was prepared using three types of particles obtained in pH 8 (sample S_pH8), pH 10 (Sample S_pH10), and pH12 (Sample S_pH12).

Ferrofluid sample having volumetric concentration of 0.25 % was inserted into test cell occupying complete volume of D1. Various voltages from 0VDC to 35 VDC as mentioned were applied to the test cell. Corresponding output voltages across R_L-C network was measured which was in the range of mV. The procedure was repeated for 0.5%, 1% and 2% volumetric concentration and corresponding V_{out} voltages were measured respectively. Above procedure was repeated for D2 and D3 test cells also. Data for cells D1, D2, D3 have been collected and tabulated in Table 2 to Table 28.

V. EXPERIMENTAL DATA

Data obtained from experimental setup has been tabulated. Table no 2 shows test result of cell D1 with ϕ = 0.25% (volumetric concentration) and particle system S_pH8 (prepared with pH-8 and particle size of 30nm). Table no.3 shows test result of cell D2 with ϕ = 0.25% and particle system S_pH8 (prepared with pH-8 and particle size of 30nm). Table no.4 shows test result of cell D3 with ϕ = 0.25% and particle system S_pH8 (prepared with pH-8 and particle size of 30nm).

Fig.12 Shows plot of Resistance vs Potential for cell D1 for particles prepared under different pH and different vol. concentrations @300K for (a) particle size of 10nm with ϕ = 0.25%,0.5%,1% and 2% ; (b) particle size of 19nm with ϕ = 0.25%,0.5%,1% and 2% and (c) particle size of 30nm with ϕ = 0.25%,0.5%,1% and 2%. Fig. 13 Shows plot of Resistance vs Potential for cell D2 for particles prepared under different pH and different vol. concentrations @300K for (a) particle size of 10nm with ϕ = 0.25%,0.5%,1% and 2%; (b) particle size of 19nm with ϕ = 0.25%,0.5%,1% and 2% and (c) particle size of 30nm with ϕ = 0.25%,0.5%,1% and 2%. Fig. 14 Shows plot of Resistance vs Potential for cell D3 for particles prepared under different pH and different vol. concentrations @300K for (a) particle size of 10nm with ϕ = 0.25%,0.5%,1% and 2%; (b) particle size of 19nm with ϕ = 0.25%,0.5%,1% and 2% and (c) particle size of 30nm with ϕ = 0.25%,0.5%,1% and 2%.

Fig.15 shows Resistance vs Potential for cells D1,D2,D3 and particles system prepared under different pH with ϕ = 0.25% @300K for (a) particle size of 10nm; (b) particle size of 19nm and (c) particle size of 30nm. Fig 16 shows Resistance vs Potential for cells D1,D2,D3 and particles system prepared under different pH with ϕ = 0.5% @300K for (a) particle size of 10nm; (b) particle size of 19nm and (c) particle size of 30nm. Fig.17 shows Resistance vs Potential

ISSN(Online) : 2319-8753
ISSN (Print) : 2347-6710

International Journal of Innovative Research in Science, Engineering and Technology

(An ISO 3297: 2007 Certified Organization)

Website: www.ijirset.com

Vol. 6, Issue 1, January 2017

for cells D1,D2,D3 and particles system prepared under different pH with ϕ = 1% @300K for (a) particle size of 10nm; (b) particle size of 19nm and (c) particle size of 30nm. Fig.18 shows Resistance vs Potential for cells D1,D2,D3 and particles system prepared under different pH with ϕ = 2% @300K for (a) particle size of 10nm; (b) particle size of 19nm and (c) particle size of 30nm.

Table no.5 shows tabulated data of resistance offered by cell D1 with variations in potentials up to 35volts with constant ϕ = 0.25% for all of the three particle systems i.e. 30nm, 19nm and 10nm. This data is plotted as per Fig.19. Table no.6 shows tabulated data of resistance offered by cell D1 with variations in potentials up to 35volts with constant ϕ = 0.5% for all of the three particle systems i.e. 30nm, 19nm and 10nm. This data is plotted as per Fig.20.Table no.7 shows tabulated data of resistance offered by cell D1 with variations in potentials up to 35volts with constant ϕ = 1% for all of the three particle systems i.e. 30nm,19nm and 10nm. This data is plotted as per Fig.21. Table no.8 shows tabulated data of resistance offered by cell D1 with variations in potentials up to 35volts with constant ϕ = 2% for all of the three particle systems i.e. 30nm, 19nm and 10nm. This data is plotted as per Fig.22.

Table no.9 shows tabulated data of resistance offered by cell D2 with variations in potentials up to 35volts with constant ϕ = 0.25% for all of the three particle systems i.e. 30nm, 19nm and 10nm. This data is plotted as per Fig.23. Table no.10 shows tabulated data of resistance offered by cell D2 with variations in potentials up to 35volts with constant ϕ = 0.5% for all of the three particle systems i.e. 30nm, 19nm and 10nm. This data is plotted as per Fig.24. Table no.11 shows tabulated data of resistance offered by cell D2 with variations in potentials up to 35volts with constant ϕ = 1% for all of the three particle systems i.e. 30nm, 19nm and 10nm. This data is plotted as per Fig.25. Table no.12 shows tabulated data of resistance offered by cell D2 with variations in potentials up to 35volts with constant ϕ = 2% for all of the three particle systems i.e. 30nm, 19nm and 10nm. This data is plotted as per Fig.26.

Table no.13 shows tabulated data of resistance offered by cell D3 with variations in potentials up to 35volts with constant ϕ = 0.25% for all of the three particle systems i.e. 30nm, 19nm and 10nm. This data is plotted as per Fig.27. Table no.14 shows tabulated data of resistance offered by cell D3 with variations in potentials up to 35volts with constant ϕ = 0.5% for all of the three particle systems i.e. 30nm, 19nm and 10nm. This data is plotted as per Fig.28. Table no.15 shows tabulated data of resistance offered by cell D3 with variations in potentials up to 35volts with constant ϕ = 1% for all of the three particle systems i.e. 30nm, 19nm and 10nm. This data is plotted as per Fig.29. Table no.16 shows tabulated data of resistance offered by cell D3 with variations in potentials up to 35volts with constant ϕ = 2% for all of the three particle systems i.e. 30nm, 19nm and 10nm. This data is plotted as per Fig.30.

Table no. 17 shows experimental analysis for cell D1 on the parameter of differential resistance obtained in changing potential from 0Volts to 35Volts i.e. change in resistance value to change in static electric field. This result was taken for ϕ = 0.25% only on ferrofluid systems of 30nm, 19nm and 10nm of particle size. Table no. 18 shows experimental analysis for cell D1 on the parameter of differential resistance obtained in changing potential from 0Volts to 35Volts i.e. change in resistance value to change in static electric field. This result was taken for ϕ = 0.5% only on ferrofluid systems of 30nm, 19nm and 10nm of particle size. Table no. 19 shows experimental analysis for cell D1 on the parameter of differential resistance obtained in changing potential from 0Volts to 35Volts i.e. change in resistance value to change in static electric field. This result was taken for ϕ = 1% only on ferrofluid systems of 30nm, 19nm and 10nm of particle size. Table no. 20 shows experimental analysis for cell D1 on the parameter of differential resistance obtained in changing potential from 0Volts to 35Volts i.e. change in resistance value to change in static electric field. This result was taken for ϕ = 2% only on ferrofluid systems of 30nm, 19nm and 10nm of particle size.

Table no. 21 shows experimental analysis for cell D2 on the parameter of differential resistance obtained in changing potential from 0Volts to 35Volts i.e. change in resistance value to change in static electric field. This result was taken for ϕ = 0.25% only on ferrofluid systems of 30nm, 19nm and 10nm of particle size. Table no. 22 shows experimental analysis for cell D2 on the parameter of differential resistance obtained in changing potential from 0Volts to 35Volts i.e. change in resistance value to change in static electric field. This result was taken for ϕ = 0.5% only on ferrofluid systems of 30nm, 19nm and 10nm of particle size. Table no. 23 shows experimental analysis for cell D2 on the parameter of differential resistance obtained in changing potential from 0Volts to 35Volts i.e. change in resistance value to change in static electric field. This result was taken for ϕ = 1% only on ferrofluid systems of 30nm, 19nm and 10nm of particle size. Table no. 24 shows experimental analysis for cell D2 on the parameter of differential resistance obtained in changing potential from 0Volts to 35Volts i.e. change in resistance value to change in static electric field. This

ISSN(Online) : 2319-8753
ISSN (Print) : 2347-6710

International Journal of Innovative Research in Science, Engineering and Technology

(An ISO 3297: 2007 Certified Organization)

Website: www.ijirset.com

Vol. 6, Issue 1, January 2017

result was taken for ϕ = 2% only on ferrofluid systems of 30nm, 19nm and 10nm of particle size.

Table no. 25 shows experimental analysis for cell D3 on the parameter of differential resistance obtained in changing potential from 0Volts to 35Volts i.e. change in resistance value to change in static electric field. This result was taken for ϕ = 0.25% only on ferrofluid systems of 30nm, 19nm and 10nm of particle size. Table no. 26 shows experimental analysis for cell D3 on the parameter of differential resistance obtained in changing potential from 0Volts to 35Volts i.e. change in resistance value to change in static electric field. This result was taken for ϕ = 0.5% only on ferrofluid systems of 30nm, 19nm and 10nm of particle size.

Table no. 27 shows experimental analysis for cell D3 on the parameter of differential resistance obtained in changing potential from 0Volts to 35Volts i.e. change in resistance value to change in static electric field. This result was taken for ϕ = 1% only on ferrofluid systems of 30nm, 19nm and 10nm of particle size. Table no. 28 shows experimental analysis for cell D3 on the parameter of differential resistance obtained in changing potential from 0Volts to 35Volts i.e. change in resistance value to change in static electric field. This result was taken for ϕ = 2% only on ferrofluid systems of 30nm, 19nm and 10nm of particle size.

Table no.5 gives details of cell D1 with ϕ = 0.25%. R_0.25 is dynamic resistance (Mega Ohm) of cell, for (S_pH12) ferrofluid system of particle having size of 10nm and dynamic resistance of cell D1 vary with Vin from 0V to 35V. Similarly, table shows dynamic resistance (Mega Ohm) for (S_pH10) ferrofluid system of particle having size of 19nm and dynamic resistance (Mega Ohm) of cell D1 for (S_pH8) ferrofluid system of particle having size of 30nm. Table no.6 gives details of cell D1 with ϕ = 0.5%. R_0.5 is dynamic resistance (Mega Ohm) of cell, for (S_pH12) ferrofluid system of particle having size of 10nm and dynamic resistance of cell D1 vary with Vin from 0V to 35V. Similarly, table shows dynamic resistance (Mega Ohm) for (S_pH10) ferrofluid system of particle having size of 19nm and dynamic resistance (Mega Ohm) of cell D1 for (S_pH8) ferrofluid system of particle having size of 30nm. Table no.7 gives details of cell D1 with ϕ = 1%. R_1 is dynamic resistance (Mega Ohm) of cell, for (S_pH12) ferrofluid system of particle having size of 10nm and dynamic resistance of cell D1 vary with Vin from 0V to 35V. Similarly, table shows dynamic resistance (Mega Ohm) for (S_pH10) ferrofluid system of particle having size of 19nm and dynamic resistance (Mega Ohm) of cell D1 for (S_pH8) ferrofluid system of particle having size of 30nm. Table no.8 gives details of cell D1 with ϕ = 2%. R_2 is dynamic resistance (Mega Ohm) of cell, for (S_pH12) ferrofluid system of particle having size of 10nm and dynamic resistance of cell D1 vary with Vin from 0V to 35V. Similarly, table shows dynamic resistance (Mega Ohm) for (S_pH10) ferrofluid system of particle having size of 19nm and dynamic resistance (Mega Ohm) of cell D1 for (S_pH8) ferrofluid system of particle having size of 30nm. Similar reading are taken for table 9 to table 12 for cell D2 and table 13 to table 16 for cell D3.

Table no.2: Test result of Cell D1 with ϕ = 0.25% (vol concentration) and particle system (S_pH8) prepared with pH-8 (As a Sample table)

Sr No	V in (V)	Diameter of cell D (m)	Area of electrode A (m^2)	Inter-electrode spacing (m)	Ratio D/A	R_L (kΩ)	Vout (mV)	Iout (nA)	R_{cell} (MΩ)	Absolute Conductivity (℧/m)	Resistivity Ω-m
1	0.0	0.026	5.3066E-04	0.003	5.65	100	0	0	274.40	2.0E-08	49.0E+06
2	5	0.026	5.3066E-04	0.003	5.65	100	4.2	42.1	118.86	4.0E-08	21.0E+06
3	10	0.026	5.3066E-04	0.003	5.65	100	11.9	119.4	83.76	6.75E-08	14.8E+06
4	15	0.026	5.3066E-04	0.003	5.65	100	22.8	228.5	65.65	8.6E-08	11.6E+06
5	20	0.026	5.3066E-04	0.003	5.65	100	34.0	339.8	58.86	9.6E-08	10.4E+06
6	25	0.026	5.3066E-04	0.003	5.65	100	47.0	469.9	53.20	10.6E-08	9.4E+06
7	30	0.026	5.3066E-04	0.003	5.65	100	58.9	588.9	50.94	11.1E-08	9.0E+06
8	35	0.026	5.3066E-04	0.003	5.65	100	75.4	754.1	46.41	12.1E-08	8.2E+06

ISSN(Online) : 2319-8753
ISSN (Print) : 2347-6710

International Journal of Innovative Research in Science, Engineering and Technology

(An ISO 3297: 2007 Certified Organization)

Website: www.ijirset.com

Vol. 6, Issue 1, January 2017

Table no 3: Test result of Cell D2 with ϕ = 0.25% (vol concentration) and particle system (S_pH8) prepared with pH-8
(As a Sample table)

Sr No	V in (V)	Diameter of cell D (m)	Area of electrode A (m^2)	Inter-electrode spacing (m)	Ratio D/A	R_L (kΩ)	Vout (mV)	Iout (nA)	R_{cell} (MΩ)	Absolute Conductivity (℧/m)	Resistivity Ω-m
1	0.0	0.026	5.3066E-04	0.006	11.31	100	0	0	282.75	4.0E-08	25.0E+06
2	5	0.026	5.3066E-04	0.006	11.31	100	3.9	39.4	126.67	8.9E-08	11.19E+06
3	10	0.026	5.3066E-04	0.006	11.31	100	11.05	110.5	90.48	12.5E-08	8.0E+06
4	15	0.026	5.3066E-04	0.006	11.31	100	22.1	221.0	67.86	16.66E-08	6.0E+06
5	20	0.026	5.3066E-04	0.006	11.31	100	32.74	327.4	61.07	18.5E-08	5.39E+06
6	25	0.026	5.3066E-04	0.006	11.31	100	42.50	425.0	58.81	19.23E-08	5.19E+06
7	30	0.026	5.3066E-04	0.006	11.31	100	53.05	530.5	56.55	20.0E-08	5.0E+06
8	35	0.026	5.3066E-04	0.006	11.31	100	64.48	644.8	54.28	20.83E-08	4.79E+06

Table no. 4: Test result of Cell D3 with ϕ = 0.25% (vol concentration) and particle system (S_pH8) prepared with pH-8
(As a Sample table)

Sr No	V in (V)	Diameter of cell D (m)	Area of electrode A (m^2)	Inter-electrode spacing (m)	Ratio D/A	R_L (kΩ)	Vout (mV)	Iout (nA)	R_{cell} (MΩ)	Absolute Conductivity (℧/m)	Resistivity Ω-m
1	0.0	0.026	5.3066E-04	0.009	16.96	100	0	0	305.28	5.0E-08	18.0E+06
2	5	0.026	5.3066E-04	0.009	16.96	100	3.0	30.7	162.81	10.41E-08	9.59E+06
3	10	0.026	5.3066E-04	0.009	16.96	100	8.9	89.3	111.93	15.17E-08	6.59E+06
4	15	0.026	5.3066E-04	0.009	16.96	100	17.6	176.8	84.80	20.0E-08	5.0E+06
5	20	0.026	5.3066E-04	0.009	16.96	100	24.5	245.7	81.40	20.83E-08	4.79E+06
6	25	0.026	5.3066E-04	0.009	16.96	100	32.0	320.4	78.01	21.74E-08	4.599E+06
7	30	0.026	5.3066E-04	0.009	16.96	100	42.1	421.17	71.23	23.81E-08	4.199E+06
8	35	0.026	5.3066E-04	0.009	16.96	100	54.3	543.0	64.44	26.31E-08	3.79E+06

ISSN(Online) : 2319-8753
ISSN (Print) : 2347-6710

International Journal of Innovative Research in Science, Engineering and Technology

(An ISO 3297: 2007 Certified Organization)

Website: www.ijirset.com

Vol. 6, Issue 1, January 2017

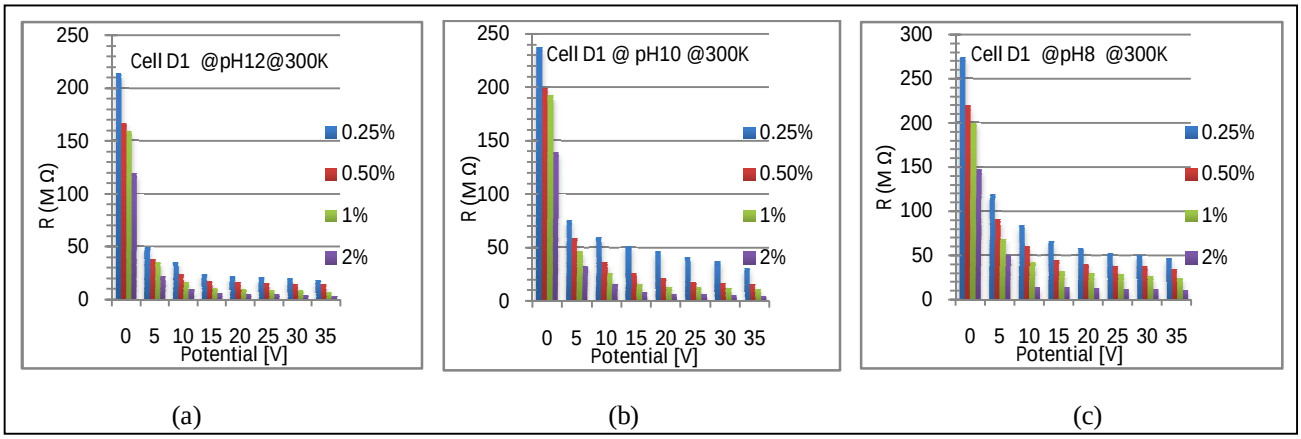

Fig. 12. Resistance vs Potential for Cell D1with different pH and different concentrations @300K
(a) particle size of 10nm with ϕ = 0.25%,0.5%,1% and 2%
(b) particle size of 19nm with ϕ = 0.25%,0.5%,1% and 2%
(c) particle size of 30nm with ϕ = 0.25%,0.5%,1% and 2%

Figure 12(a), 12(b), 12(c) shows that in cell D1, resistance of ferrofluid decreases with increase in volumetric concentration. It can also be observed that resistance increases with increase in particle size. Increase in resistance amounts to decrease in electrical conductivity and vice versa.

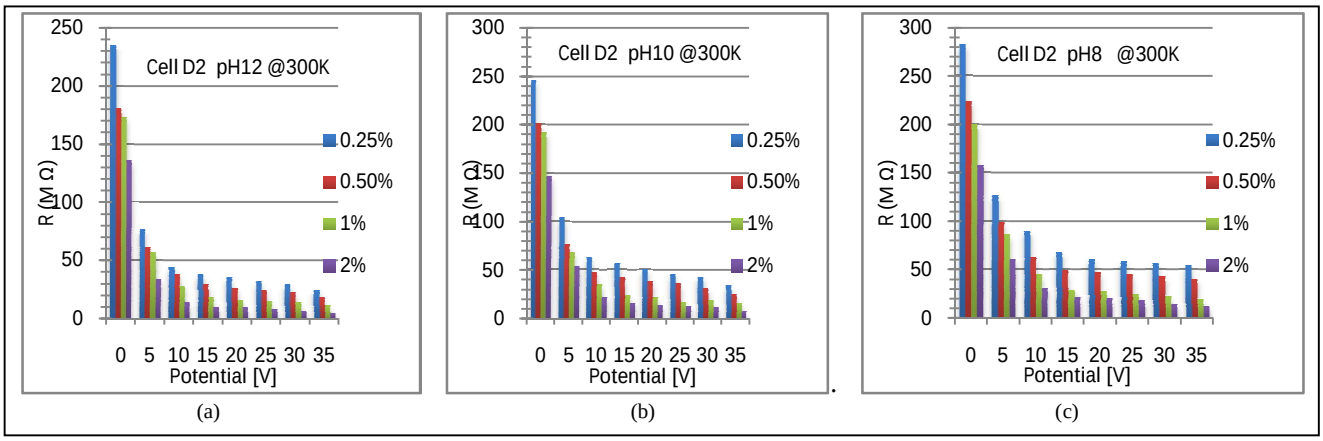

Fig. 13. Resistance vs Potential for Cell D2with different pH and different concentrations @300K
(a) particle size of 10nm with ϕ = 0.25%,0.5%,1% and 2%
(b) particle size of 19nm with ϕ = 0.25%,0.5%,1% and 2%
(c) particle size of 30nm with ϕ = 0.25%,0.5%,1% and 2%

Figure 13(a), 13(b), 13(c) shows that in cell D2, resistance of ferrofluid decreases with increase in volumetric concentration. It can also be observed that resistance increases with increase in particle size. Increase in resistance amounts to decrease in electrical conductivity and vice versa.

ISSN(Online) : 2319-8753
ISSN (Print) : 2347-6710

International Journal of Innovative Research in Science, Engineering and Technology

(An ISO 3297: 2007 Certified Organization)

Website: www.ijirset.com

Vol. 6, Issue 1, January 2017

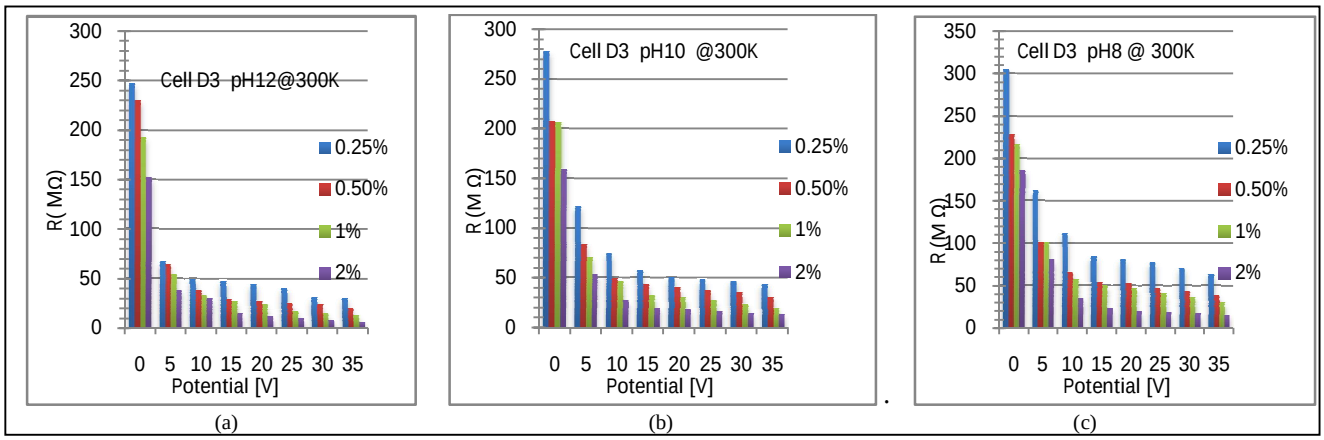

Fig. 14. Resistance vs Potential for Cell D3with different pH and different concentrations @300K
(a) Particle size of 10nm with ϕ = 0.25%,0.5%,1% and 2%
(b) Particle size of 19nm with ϕ = 0.25%,0.5%,1% and 2%
(c) Particle size of 30nm with ϕ = 0.25%,0.5%,1% and 2%

Figure 14(a), 14(b), 14(c) shows that in cell D3, resistance of ferrofluid decreases with increase in volumetric concentration. It can also be observed that resistance increases with increase in particle size. Increase in resistance amounts to decrease in electrical conductivity and vice versa.

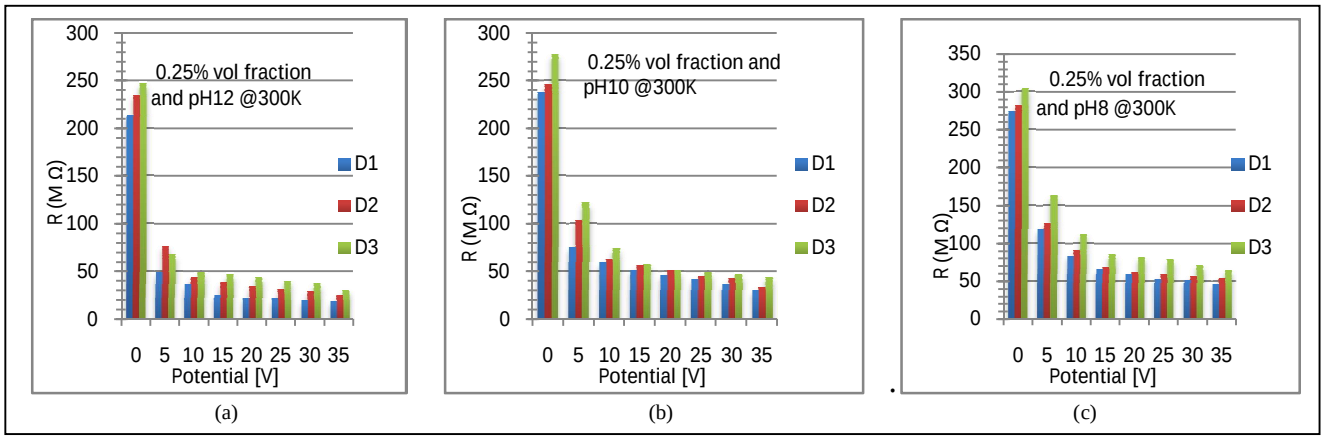

Fig. 15. Resistance vs Potential for cells D1,D2,D3 and different pH with ϕ = 0.25% @300K
(a) particle size of 10nm, (b) particle size of 19nm, (c) particle size of 30nm

Figure 15(a), 15(b), 15(c) shows that in cell D1, D2, and D3 with 0.25% concentration, there is no appreciable change in conductivity of ferrofluid. Inter-electrode spacings of all these test cells (D1, D2, D3) are different and these dimensions have no influence on changing electrical conductivity of ferrofluid.

ISSN(Online) : 2319-8753
ISSN (Print) : 2347-6710

International Journal of Innovative Research in Science, Engineering and Technology

(An ISO 3297: 2007 Certified Organization)

Website: www.ijirset.com

Vol. 6, Issue 1, January 2017

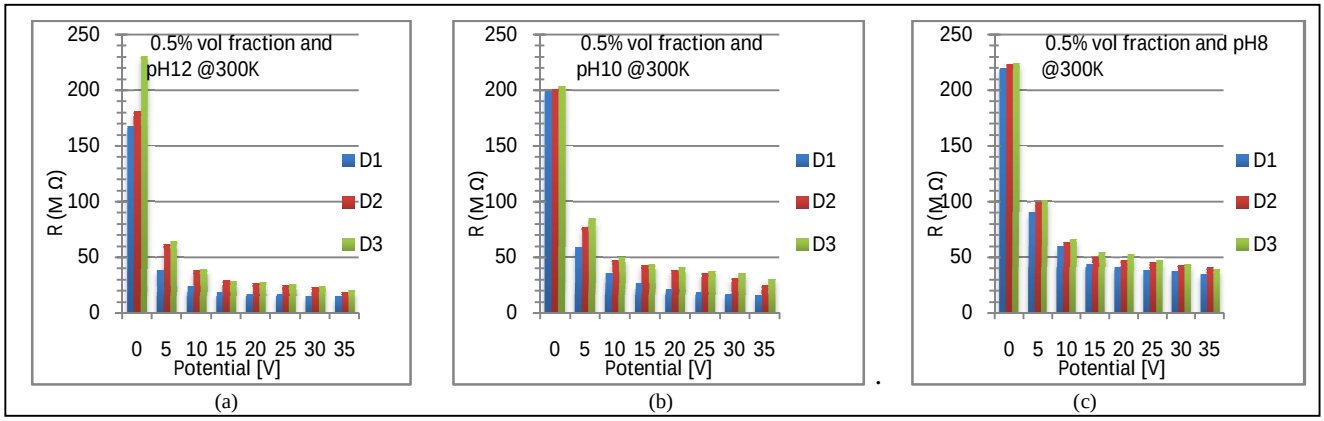

Fig. 16. Resistance vs Potential for cells D1,D2,D3 and different pH with ϕ = 0.5% @300K
(a) particle size of 10nm, (b) particle size of 19nm, (c) particle size of 30nm

Figure 16(a), 16(b), 16(c) shows that in cell D1, D2, and D3 with 0.5% concentration, there is no appreciable change in conductivity of ferrofluid. Inter-electrode spacings of all these test cells (D1, D2, D3) are different and these dimensions have no influence on changing electrical conductivity of ferrofluid.

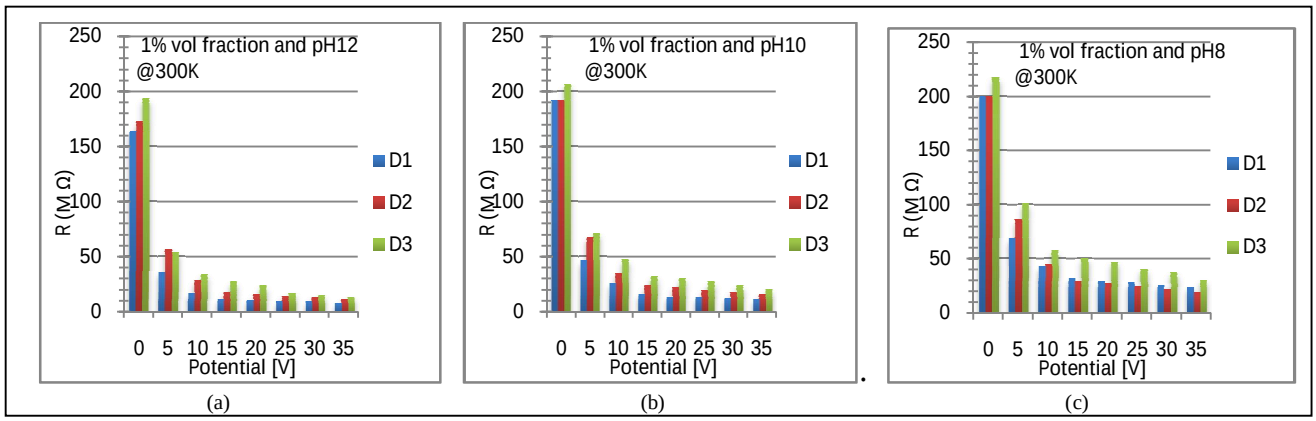

Fig. 17. Resistance vs Potential for cells D1,D2,D3 and different pH with ϕ = 1% @300K
(a) particle size of 10nm, (b) particle size of 19nm, (c) particle size of 30nm

Figure 17(a), 17(b), 17(c) shows that in cell D1, D2, and D3 with 1% concentration, there is no appreciable change in conductivity of ferrofluid. Inter-electrode spacing of all these test cells (D1, D2, D3) are different and these dimensions have no influence on changing electrical conductivity of ferrofluid.

ISSN(Online) : 2319-8753
ISSN (Print) : 2347-6710

International Journal of Innovative Research in Science, Engineering and Technology

(An ISO 3297: 2007 Certified Organization)

Website: www.ijirset.com

Vol. 6, Issue 1, January 2017

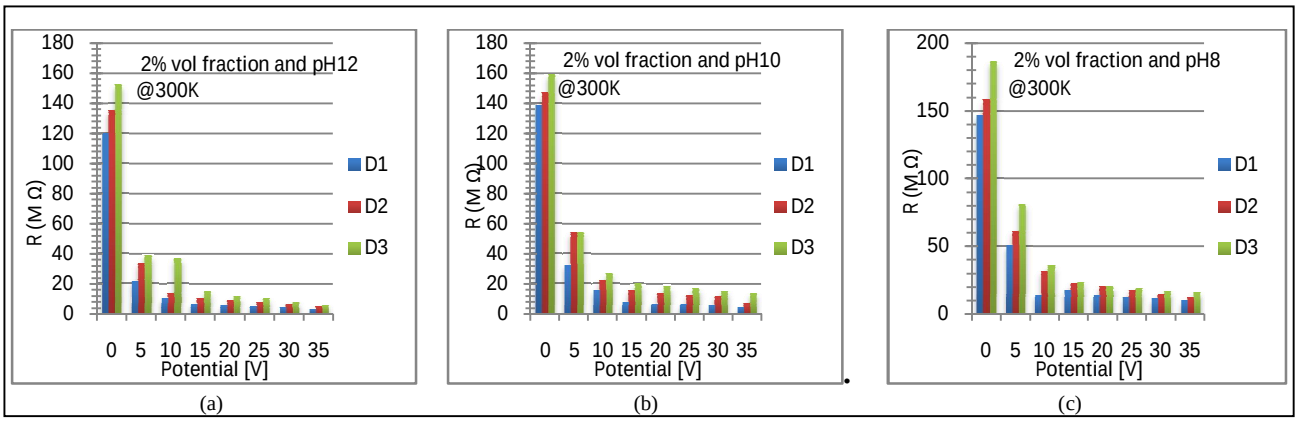

Fig. 18. Resistance vs Potential for cells D1,D2,D3 and different pH with ϕ = 2% @300K
(a) particle size of 10nm, (b) particle size of 19nm, (c) particle size of 30nm

Figure 18(a), 18(b), 18(c) shows that in cell D1, D2, and D3 with 2% concentration, there is no appreciable change in conductivity of ferrofluid. Inter-electrode spacings of all these test cells (D1, D2, and D3) are different and these dimensions have no influence on changing electrical conductivity of ferrofluid.

Table no.5: Cell D1 with ϕ = 0.25%

V in (V)	(S_pH12) R_0.25 MΩ	(S_pH10) R_0.25 MΩ	(S_pH8) R_0.25 MΩ
0.0	213.9	237.72	274.00
5	49.8	75.84	118.86
10	36.22	59.99	83.76
15	24.9	52.07	65.65
20	22.64	46.41	58.86
25	21.5	41.88	53.20
30	20.37	37.35	50.94
35	19.24	30.56	46.41

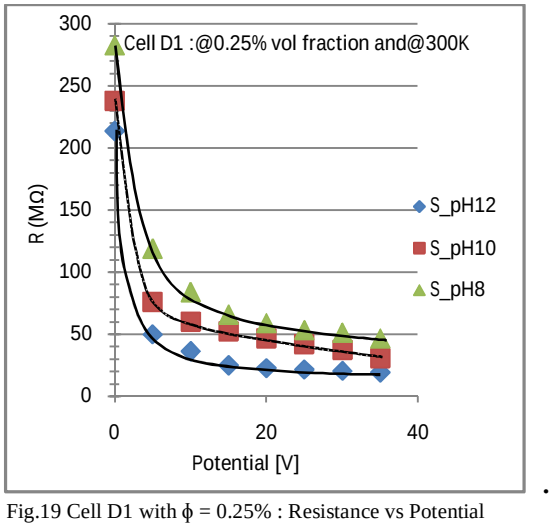

Fig.19 Cell D1 with ϕ = 0.25% : Resistance vs Potential

Table no.5 shows variation in resistance offered by cell D1 with 0.25% volumetric concentration. Fig 19 shows variation in resistance against variations in potential up to 35volts for all particle systems i.e. 30nm, 19nm and 10nm. From graphical presentation, it can be observed that, resistance decreases with increase in inter electrode potential. This is true for all three particle systems. It can also be inferred that for a given static potential, resistance was found to increase with increasing particle size in ferrofluid.

ISSN(Online) : 2319-8753
ISSN (Print) : 2347-6710

International Journal of Innovative Research in Science, Engineering and Technology

(An ISO 3297: 2007 Certified Organization)

Website: www.ijirset.com

Vol. 6, Issue 1, January 2017

Table no.6: Cell D1 with ϕ=0.50%

V in (V)	(S_pH12) R_0.5 MΩ	(S_pH10) R_0.5 MΩ	(S_pH8) R_0.5 MΩ
0	167.53	199.23	219.6
5	38.48	58.86	90.56
10	23.77	36.22	59.99
15	18.11	26.03	44.14
20	16.98	21.5	40.75
25	16.41	18.11	38.48
30	15.28	16.98	37.35
35	14.71	15.84	35.092

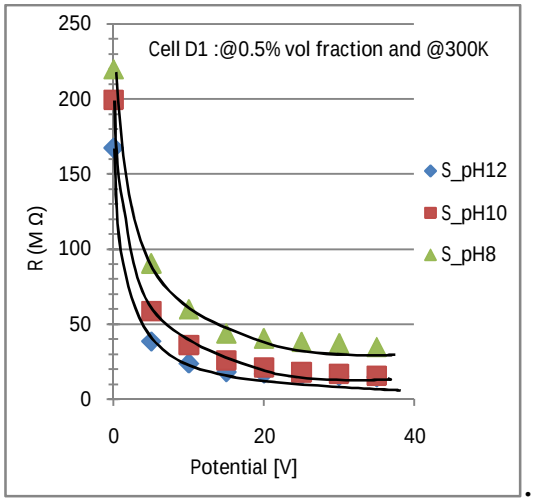

Fig.20 Cell D1: ϕ= 0.5% Potential vs Resistance

Table no.6 shows variation in resistance offered by cell D1 with 0.5% volumetric concentration. Fig 20 shows variation in resistance against variations in potential up to 35volts for all particle systems i.e. 30nm, 19nm and 10nm. From graphical presentation, it can be observed that, resistance decreases with increase in inter electrode potential. This is true for all three particle systems. It can also be inferred that for a given static potential, resistance was found to increase with increasing particle size in ferrofluid.

Table no.7: Cell D1 with ϕ=1%

V in (V)	(S_pH12) R_1 MΩ	(S_pH10) R_1 MΩ	(S_pH8) R_1 MΩ
0	159.14	192.4	200.36
5	36.22	46.41	69.05
10	16.98	26.03	43.016
15	11.43	15.84	31.69
20	10.69	13.58	29.43
25	9.62	13.01	28.3
30	9.33	12.45	26.036
35	7.92	11.32	18.77

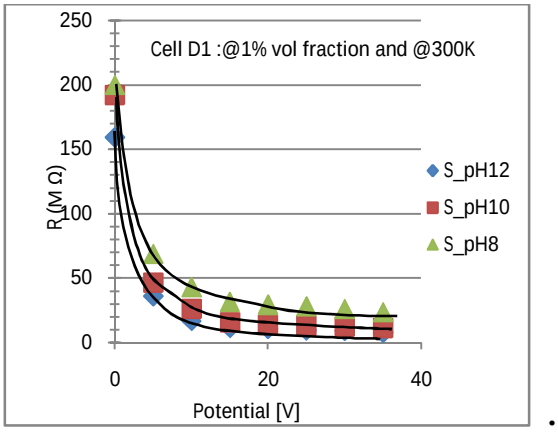

Fig.21 Cell D1: ϕ=1% Potential vs Resistance

Table no.7 shows variation in resistance offered by cell D1 with 1% volumetric concentration. Fig 21 shows variation in resistance against variations in potential up to 35volts for all particle systems i.e. 30nm, 19nm and 10nm. From graphical presentation, it can be observed that, resistance decreases with increase in inter electrode potential. This is true for all three particle systems. It can also be inferred that for a given static potential, resistance was found to increase with increasing particle size in ferrofluid.

ISSN(Online) : 2319-8753
ISSN (Print) : 2347-6710

International Journal of Innovative Research in Science, Engineering and Technology

(An ISO 3297: 2007 Certified Organization)

Website: www.ijirset.com

Vol. 6, Issue 1, January 2017

Table no.8: Cell D1 with ϕ= 2%

V in (V)	(S_pH12) R_2 MΩ	(S_pH10) R_2 MΩ	(S_pH8) R_2 MΩ
0	119.9	139.23	147.16
5	22.07	32.82	50.94
10	10.75	15.84	22.15
15	6.79	7.92	17.54
20	5.66	6.79	13.58
25	5.54	6.16	12.45
30	4.52	5.66	11.32
35	3.39	4.52	10.18

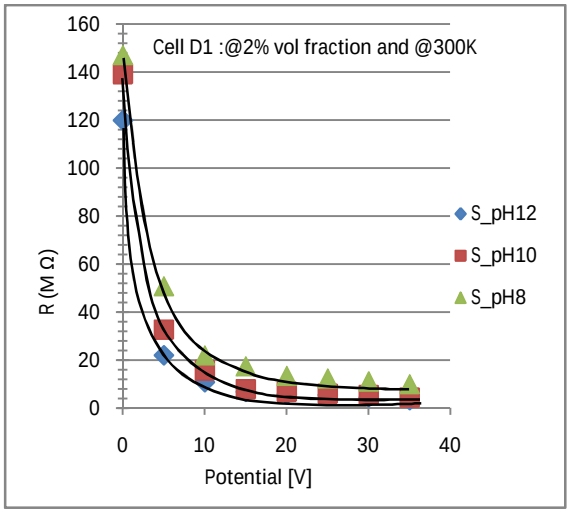

Fig.22 Cell D1: ϕ=2% Potential vs Resistance

Table no.8 shows variation in resistance offered by cell D1 with 2% volumetric concentration. Fig 22 shows variation in resistance against variations in potential up to 35volts for all particle systems i.e. 30nm, 19nm and 10nm. From graphical presentation, it can be observed that, resistance decreases with increase in inter electrode potential. This is true for all three particle systems. It can also be inferred that for a given static potential, resistance was found to increase with increasing particle size in ferrofluid.

Table no.9: Cell D2 with ϕ=0.25%

V in (V)	(S_pH12) R_0.25 MΩ	(S_pH10) R_0.25 MΩ	(S_pH8) R_0.25 MΩ
0	235.24	246.55	282.75
5	76.90	104.05	126.67
10	44.10	63.33	90.48
15	38.45	56.55	67.86
20	35.06	50.89	61.07
25	31.66	45.24	58.81
30	29.40	42.97	56.55
35	24.88	34.04	54.28

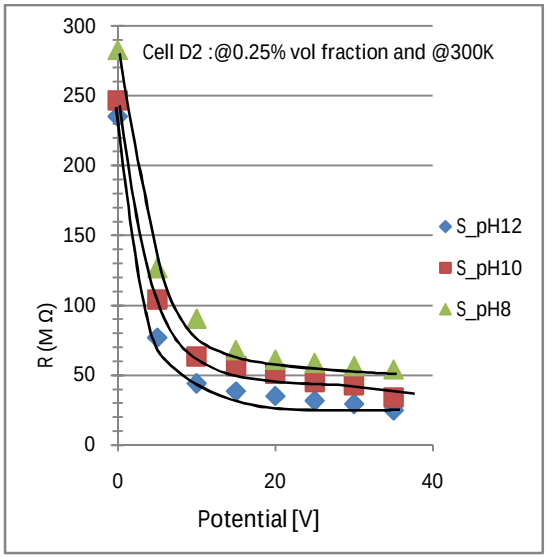

Fig.23 Cell D2: ϕ= 0.25% Potential vs Resistance

ISSN(Online) : 2319-8753
ISSN (Print) : 2347-6710

International Journal of Innovative Research in Science, Engineering and Technology

(An ISO 3297: 2007 Certified Organization)

Website: www.ijirset.com

Vol. 6, Issue 1, January 2017

Table no.9 shows variation in resistance offered by cell D2 with 0.25% volumetric concentration. Fig 23 shows variation in resistance against variations in potential up to 35volts for all particle systems i.e. 30nm, 19nm and 10nm. From graphical presentation, it can be observed that, resistance decreases with increase in inter electrode potential. This is true for all three particle systems. It can also be inferred that for a given static potential, resistance was found to increase with increasing particle size in ferrofluid.

Table no.10: Cell D2 with ϕ=0.5%

V in (V)	(S_pH12) R_0.5 MΩ	(S_pH10) R_0.5 MΩ	(S_pH8) R_0.5 MΩ
0	180.96	201.31	223.62
5	61.07	76.90	99.52
10	38.45	47.50	63.33
15	29.4	42.97	49.76
20	26.01	38.45	47.5
25	24.88	36.19	45.24
30	22.62	31.66	42.97
35	18.096	24.88	40.71

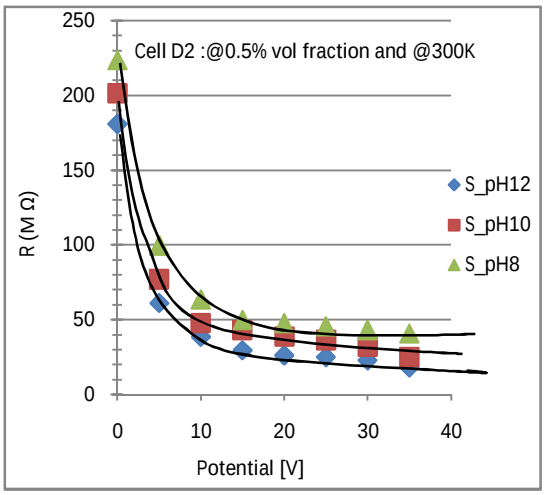

Fig.24. Cell D2: ϕ=0.5% Potential vs Resistance

Table no.10 shows variation in resistance offered by cell D2 with 0.5% volumetric concentration. Fig 24 shows variation in resistance against variations in potential up to 35volts for all particle systems i.e. 30nm, 19nm and 10nm. From graphical presentation, it can be observed that, resistance decreases with increase in inter electrode potential. This is true for all three particle systems. It can also be inferred that for a given static potential, resistance was found to increase with increasing particle size in ferrofluid.

Table no.11: Cell D2 with ϕ=1%

V in (V)	(S_pH12) R_1 MΩ	(S_pH10) R_1 MΩ	(S_pH8) R_1 MΩ
0	173.22	192.27	200.29
5	56.55	67.86	85.95
10	28.27	35.06	45.24
15	18.09	23.75	29.40
20	15.82	22.62	27.14
25	14.70	19.22	24.88
30	13.57	18.09	22.62
35	11.31	15.83	19.22

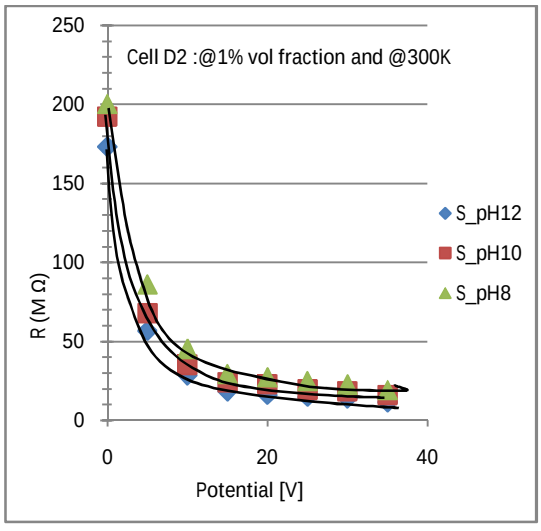

Fig.25. Cell D2: ϕ=1% Potential vs Resistance

ISSN(Online) : 2319-8753
ISSN (Print) : 2347-6710

International Journal of Innovative Research in Science, Engineering and Technology

(An ISO 3297: 2007 Certified Organization)

Website: www.ijirset.com

Vol. 6, Issue 1, January 2017

Table no.11 shows variation in resistance offered by cell D2 with 1% volumetric concentration. Fig 25 shows variation in resistance against variations in potential up to 35volts for all particle systems i.e. 30nm, 19nm and 10nm. From graphical presentation, it can be observed that, resistance decreases with increase in inter electrode potential. This is true for all three particle systems. It can also be inferred that for a given static potential, resistance was found to increase with increasing particle size in ferrofluid.

Table no.12: Cell D2 with ϕ=2%

V in (V)	(S_pH12) R_2 MΩ	(S_pH10) R_2 MΩ	(S_pH8) R_2 MΩ
0	135.72	137.98	158.34
5	33.93	54.28	61.07
10	13.57	22.62	31.66
15	10.06	15.83	22.62
20	9.048	13.57	20.35
25	7.917	12.44	18.09
30	6.786	11.98	14.70
35	5.089	7.01	12.44

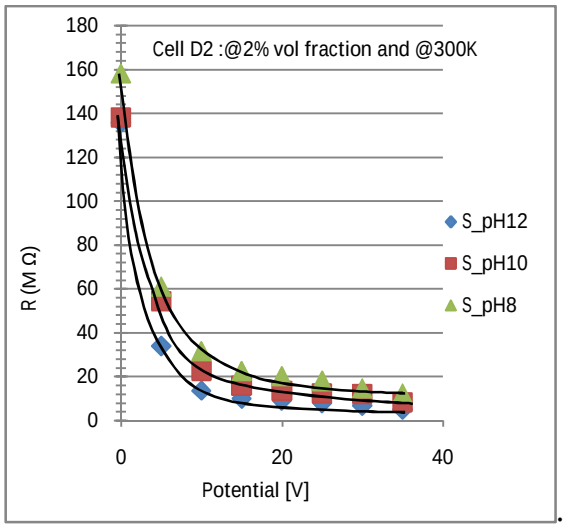

Fig.26. Cell D2: ϕ=2% Potential vs Resistance

Table no.12 shows variation in resistance offered by cell D2 with 2% volumetric concentration. Fig 26 shows variation in resistance against variations in potential up to 35volts for all particle systems i.e. 30nm, 19nm and 10nm. From graphical presentation, it can be observed that, resistance decreases with increase in inter electrode potential. This is true for all three particle systems. It can also be inferred that for a given static potential, resistance was found to increase with increasing particle size in ferrofluid.

Table no.13: Cell D3 ϕ=0.25%

V in (V)	(S_pH12) R_0.25 MΩ	(S_pH10) R_0.25 MΩ	(S_pH8) R_0.25 MΩ
0	247.61	278.14	305.28
5	67.84	122.11	162.81
10	49.18	74.62	111.93
15	47.48	57.66	84.80
20	44.40	50.88	81.40
25	40.70	49.01	78.01
30	37.71	47.48	71.23
35	30.52	44.09	64.44

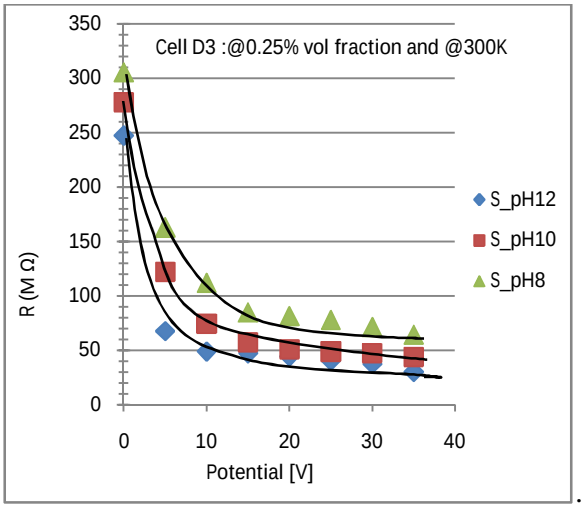

Fig.27. Cell D3: ϕ=0.25% Potential vs Resistance

ISSN(Online) : 2319-8753
ISSN (Print) : 2347-6710

International Journal of Innovative Research in Science, Engineering and Technology

(An ISO 3297: 2007 Certified Organization)

Website: www.ijirset.com

Vol. 6, Issue 1, January 2017

Table no.13 shows variation in resistance offered by cell D3 with 0.25% volumetric concentration. Fig 27 shows variation in resistance against variations in potential up to 35volts for all particle systems i.e. 30nm, 19nm and 10nm. From graphical presentation, it can be observed that, resistance decreases with increase in inter electrode potential. This is true for all three particle systems. It can also be inferred that for a given static potential, resistance was found to increase with increasing particle size in ferrofluid.

Table no.14: Cell D3 ϕ=0.5%

V in (V)	(S_pH12) R_0.5 MΩ	(S_pH10) R_0.5 MΩ	(S_pH8) R_0.5 MΩ
0	189.95	203.52	228.87
5	64.44	84.80	101.76
10	39.00	49.84	66.44
15	28.83	44.00	54.27
20	27.13	40.70	52.57
25	25.44	37.31	47.48
30	23.74	35.61	43.75
35	20.35	30.52	39.00

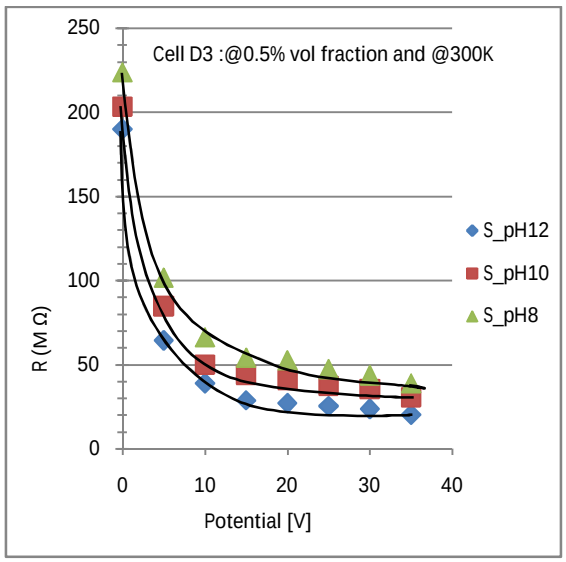

Fig.28 Cell D3: ϕ=0.5% Potential vs Resistance

Table no.14 shows variation in resistance offered by cell D3 with 0.5% volumetric concentration. Fig 28 shows variation in resistance against variations in potential up to 35volts for all particle systems i.e. 30nm, 19nm and 10nm. From graphical presentation, it can be observed that, resistance decreases with increase in inter electrode potential. This is true for all three particle systems. It can also be inferred that for a given static potential, resistance was found to increase with increasing particle size in ferrofluid.

Table no.15: Cell D3 ϕ=1%

V in (V)	(S_pH12) R_1 MΩ	(S_pH10) R_1 MΩ	(S_pH8) R_1 MΩ
0	193.34	206.91	217.26
5	54.27	71.23	101.76
10	33.92	47.48	57.66
15	27.13	32.22	50.88
20	23.74	30.52	47.48
25	16.96	27.13	40.70
30	15.26	23.74	37.31
35	13.56	20.35	30.52

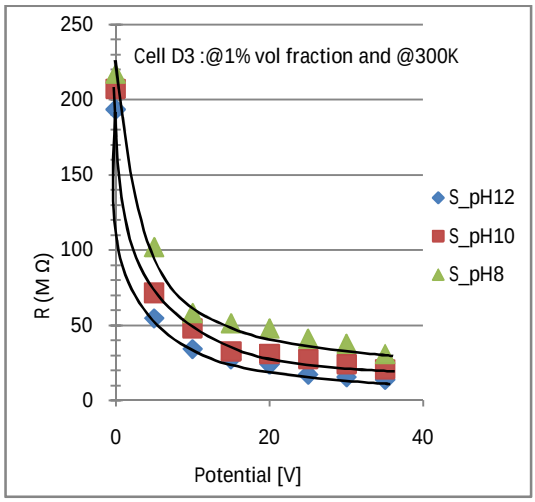

Fig.29 Cell D3: ϕ= 1% Potential vs Resistance

ISSN(Online) : 2319-8753
ISSN (Print) : 2347-6710

International Journal of Innovative Research in Science, Engineering and Technology

(An ISO 3297: 2007 Certified Organization)

Website: www.ijirset.com

Vol. 6, Issue 1, January 2017

Table no.15 shows variation in resistance offered by cell D3 with 1% volumetric concentration. Fig 29 shows variation in resistance against variations in potential up to 35volts for all particle systems i.e. 30nm, 19nm and 10nm. From graphical presentation, it can be observed that, resistance decreases with increase in inter electrode potential. This is true for all three particle systems. It can also be inferred that for a given static potential, resistance was found to increase with increasing particle size in ferrofluid.

Table no.16: Cell D3: ϕ=2%

V in (V)	(S_pH12) R_2 MΩ	(S_pH10) R_2 MΩ	(S_pH8) R_2 MΩ
0	152.64	159.42	186.56
5	39.0	54.27	81.40
10	27.31	40.7	44.41
15	15.26	20.35	23.74
20	11.87	18.65	20.35
25	10.17	16.96	18.65
30	8.14	15.26	16.96
35	6.936	13.56	16.11

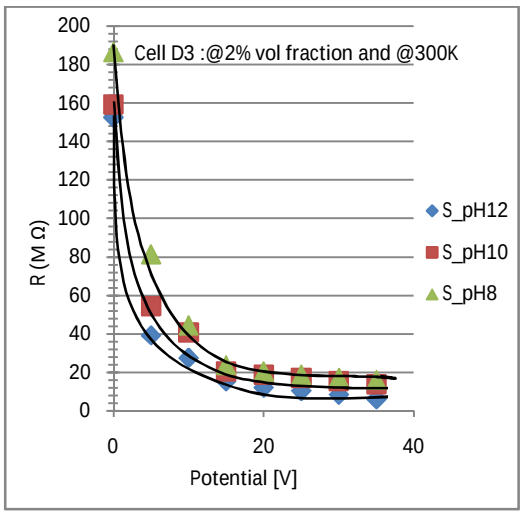

Fig.30 Cell D2: ϕ=2% Potential vs Resistance

Table no.16 shows variation in resistance offered by cell D3 with 2% volumetric concentration. Fig 30 shows variation in resistance against variations in potential up to 35volts for all particle systems i.e. 30nm, 19nm and 10nm. From graphical presentation, it can be observed that, resistance decreases with increase in inter electrode potential. This is true for all three particle systems. It can also be inferred that for a given static potential, resistance was found to increase with increasing particle size in ferrofluid.

A. EXPERIMENTAL ANALYSIS OF DIFFERENTIAL RESPONSE TO STATIC ELECTRIC FIELD ON CELL D1

a. Table no.17: With 0.25% volume concentration

D_{TEM}	M_{VSM} (emu/cc)	R @ V=0 V (MΩ)	R@V=35V (MΩ)	Δ(R @ 0V – R@35V)
10	82.21	213.9	19.24	194.66
19	76.0	237.72	30.56	207.16
30	63.5	274.0	46.41	227.59

b. Table no.18 : With 0.5% volume concentration

D_{TEM}	M_{VSM} (emu/cc)	R @ V= 0 V (MΩ)	R @ V=35V (MΩ)	Δ(R @0V - R @ 35V)
10	82.21	167.53	14.71	152.82
19	76.0	199.23	15.84	183.39
30	63.5	219.9	35.09	184.51

ISSN(Online) : 2319-8753
ISSN (Print) : 2347-6710

International Journal of Innovative Research in Science, Engineering and Technology

(An ISO 3297: 2007 Certified Organization)

Website: www.ijirset.com

Vol. 6, Issue 1, January 2017

Table no. 17 shows experimental analysis for cell D1 on the parameter of differential resistance obtained in changing potential from 0Volts to 35Volts i.e. change in resistance value to change in static electric field. This result was taken for ϕ = 0.25% only on ferrofluid systems of 30nm, 19nm and 10nm of particle size. As the particle size increase change in resistance value was increase.

Table no. 18 shows experimental analysis for cell D1 on the parameter of differential resistance obtained in changing potential from 0Volts to 35Volts i.e. change in resistance value to change in static electric field. This result was taken for ϕ = 0.5% only on ferrofluid systems of 30nm, 19nm and 10nm of particle size. As the particle size increase change in resistance value was increase.

c. Table no.19: With 1% volume concentration

D_{TEM}	M_{VSM} (emu/cc)	R@ V=0V (MΩ)	R@ V=35V (MΩ)	Δ(R @0V - R @ 35V)
10	82.21	159.14	7.92	151.22
19	76.0	192.4	11.32	181.08
30	63.5	200.36	18.77	181.59

d. Table no.20: With 2% volume concentration

D_{TEM}	M_{VSM} (emu/cc)	R @ V=0 V (MΩ)	R @ V=35V (MΩ)	Δ(R @ 0V - R @ 35V)
10	82.21	119.9	3.39	116.51
19	76.0	139.23	4.52	134.48
30	63.5	147.16	10.18	136.98

Table no. 19 shows experimental analysis for cell D1 on the parameter of differential resistance obtained in changing potential from 0Volts to 35Volts i.e. change in resistance value to change in static electric field. This result was taken for ϕ = 1% only on ferrofluid systems of 30nm, 19nm and 10nm of particle size. As the particle size increase change in resistance value was increase.

Table no. 20 shows experimental analysis for cell D1 on the parameter of differential resistance obtained in changing potential from 0Volts to 35Volts i.e. change in resistance value to change in static electric field. This result was taken for ϕ = 2% only on ferrofluid systems of 30nm, 19nm and 10nm of particle size. As the particle size increase change in resistance value was increase.

B. Experimental analysis of differential response to static electric field on cell D2

a. Table no.21: With 0.25% volume concentration.

D_{TEM}	M_{VSM} (emu/cc)	R @V=0V (MΩ)	R@=35V (MΩ)	Δ(R @ 0V - R @ 35V)
10	82.21	235.24	24.88	210.6
19	76.0	246.55	34.043	212.51
30	63.5	282.75	54.28	228.47

b. Table no.22: With 0.5% volume concentration

D_{TEM}	M_{VSM} (emu/cc)	R @ V=0 V (MΩ)	R@ V=35V (MΩ)	Δ(R @ 0V - R @ 35V)
10	82.21	180.96	18.09	162.87
19	76.0	201.31	24.88	176.43
30	63.5	223.62	40.71	182.91

Table no. 21 shows experimental analysis for cell D2 on the parameter of differential resistance obtained in changing

ISSN(Online) : 2319-8753
ISSN (Print) : 2347-6710

International Journal of Innovative Research in Science, Engineering and Technology

(An ISO 3297: 2007 Certified Organization)

Website: www.ijirset.com

Vol. 6, Issue 1, January 2017

potential from 0Volts to 35Volts i.e. change in resistance value to change in static electric field. This result was taken for ϕ = 0.25% only on ferrofluid systems of 30nm, 19nm and 10nm of particle size.

Table no. 22 shows experimental analysis for cell D2 on the parameter of differential resistance obtained in changing potential from 0Volts to 35Volts i.e. change in resistance value to change in static electric field. This result was taken for ϕ = 0.5% only on ferrofluid systems of 30nm, 19nm and 10nm of particle size.

c. Table no.23: With 1% volume concentration

D_{TEM}	M_{VSM} (emu/cc)	R @ V=0 V (MΩ)	R@ V=35V (MΩ)	Δ(R @ V - R @ 2V)
10	82.21	173.22	11.31	161.91
19	76.0	192.27	15.83	176.44
30	63.5	200.29	19.22	181.07

d. Table no.24: With 2% volume concentration

D_{TEM}	M_{VSM} (emu/cc)	R @ V=0 V (MΩ)	R @ V=35V (MΩ)	Δ(R @ 0V - R @ 35V)
10	82.21	135.72	5.08	130.61
19	76.0	137.98	11.31	131.97
30	63.5	158.34	12.44	145.9

Table no. 23 shows experimental analysis for cell D2 on the parameter of differential resistance obtained in changing potential from 0Volts to 35Volts i.e. change in resistance value to change in static electric field. This result was taken for ϕ = 1% only on ferrofluid systems of 30nm, 19nm and 10nm of particle size.

Table no. 24 shows experimental analysis for cell D2 on the parameter of differential resistance obtained in changing potential from 0Volts to 35Volts i.e. change in resistance value to change in static electric field. This result was taken for ϕ = 2% only on ferrofluid systems of 30nm, 19nm and 10nm of particle size.

C. *EXPERIMENTAL ANALYSIS OF DIFFERENTIAL RESPONSE TO STATIC ELECTRIC FIELD ON CELL D3.*

a. Table no.25: With 0.25% volume concentration

D_{TEM}	M_{VSM} (emu/cc)	R@ V=0 V (MΩ)	R@ V=35V (MΩ)	Δ(R @ 0V - R @ 35V)
10	82.21	247.61	30.52	217.09
19	76.0	278.14	44.09	234.05
30	63.5	305.28	64.44	240.84

b. Table no.26: With 0.5% volume concentration

D_{TEM}	M_{VSM} (emu/cc)	R @ V=0 V (MΩ)	R@ V=35V (MΩ)	Δ(R @ 0V - R @ 35V)
10	82.21	189.95	20.35	169.6
19	76.0	203.52	30.52	173.0
30	63.5	228.87	39.00	189.87

Table no. 25 shows experimental analysis for cell D3 on the parameter of differential resistance obtained in changing potential from 0Volts to 35Volts i.e. change in resistance value to change in static electric field. This result was taken for ϕ = 0.25% only on ferrofluid systems of 30nm, 19nm and 10nm of particle size. Table no. 26 shows experimental analysis for cell D3 on the parameter of differential resistance obtained in changing potential from 0Volts to 35Volts i.e.

ISSN(Online) : 2319-8753
ISSN (Print) : 2347-6710

International Journal of Innovative Research in Science, Engineering and Technology

(An ISO 3297: 2007 Certified Organization)

Website: www.ijirset.com

Vol. 6, Issue 1, January 2017

change in resistance value to change in static electric field. This result was taken for ϕ = 0.5% only on ferrofluid systems of 30nm, 19nm and 10nm of particle size.

c. Table no.27: With 1% volume concentration

D_{TEM}	M_{VSM} (emu/cc)	R@ V=0 V (MΩ)	R @ V=35V (MΩ)	Δ(R @ 0V-R@ 35V)
10	82.21	193.34	13.56	179.78
19	76.0	206.91	20.35	186.56
30	63.5	217.26	30.52	187.74

d. Table no.28: With 2% volume concentration

D_{TEM}	M_{VSM} (emu/cc)	R@ V=0 V (MΩ)	R@ V=35V (MΩ)	Δ(R @ 0V - R @ 35V)
10	82.21	152.64	5.93	145.71
19	76.0	159.42	13.56	145.86
30	63.5	186.56	16.11	170.45

Table no. 27 shows experimental analysis for cell D3 on the parameter of differential resistance obtained in changing potential from 0Volts to 35Volts i.e. change in resistance value to change in static electric field. This result was taken for ϕ = 1% only on ferrofluid systems of 30nm, 19nm and 10nm of particle size.
Table no. 28 shows experimental analysis for cell D3 on the parameter of differential resistance obtained in changing potential from 0Volts to 35Volts i.e. change in resistance value to change in static electric field. This result was taken for ϕ = 2% only on ferrofluid systems of 30nm, 19nm and 10nm of particle size

VI. RESULTS AND DISCUSSIONS

Magnetite powder was dried in oven for 24 Hrs with 80^{O}C and XRD was taken on Philips make X'pert PRO model. The size of the crystal is calculated by Scherer's formula as follows. XRD wavelength λ of 0.15406 nm was used for characterization. The value of K is 0.89 for magnetite and θ is bragg's angle.

$$D=K\lambda/(B\cos\theta)$$

B is a full width half maximum (FWHM), The largest intensity in the graph is at [311] plane with 2θ of 35.7^{o}. Half maximum intensity width of the peak accounted with instrument broadening, particle sizes were calculated to be 29.6nm, 18.7nm and 9.2nm (Fig. 1,2,3).The TEM of the system are shown in the Fig. 4,Fig 5,Fig 6.

JEOL make TEM instrument Model-JEM 2100 was used for characterisation of nano material. Required evacuation current was below 64 micro amperes for TEM to work under safety limit. TEM images have been taken below 32 micro amperes so that filament of TEM is safe. At such a small filament current, the beam voltage was set at 200 KV and maximum beam current of 98 micrro amperes was observed. During image extraction only 3 to 4 micro amperes of beam current have been observed to increase. TEM images of ferrimagnetic particles synthesized at different pH of 8, 10 and 12 have been taken. The size of ferrimagnetic particles synthesized at different pH of 8, 10 and 12 were observed as 30nm, 19nm and 10nm respectively. The diameter of nano particle observed on TEM and calculated from XRD data is tabulated in Table 1.

Magentisation (M) vs Field (H) for Fe_3O_4 nano particles at 300K was carried out and shown as Fig 7. M–H curve for the different magnetite sample (30nm,19nm,10nm) were shown. In the presence of a magnetic field H, the magnetic moment (μ) of the particles tends to magnetize. They try to align in the direction with the external magnetic field. The hysteresis depends upon the magnetic domain walls at impurities or grain boundaries within the material and the magnetic anisotropy of the crystalline lattice. Particle size also affects the shape of these loops. Super paramagnetic

ISSN(Online) : 2319-8753
ISSN (Print) : 2347-6710

International Journal of Innovative Research in Science, Engineering and Technology

(An ISO 3297: 2007 Certified Organization)

Website: www.ijirset.com

Vol. 6, Issue 1, January 2017

behaviour was observed at smaller size particles as compared to other particles having size of 19 and 30 nm. The obtained saturation magnetization (M_{sat}) for magnetite sample synthesized at different pH (8, 10 and 12) at room temperature were 82.21 emu/cc, 76.0emu/cc and 63.5 emu/cc respectively. When magnetic nanoparticles are suspended in kerosene steric repulsion produced between particles due to surface treatment by oleic acid avoids the formation of agglomeration. These ferrimagnetic particles behave like a single domain particles with super paramagnetic behaviour.

The FTIR spectrum shows absorption band at 1710cm^{-1} which presents the stretching vibration of the carboxyl group (C = O), associated to the oleic acid molecule, adsorbed on to the surface of the crystallites. FTIR spectrum in fig 8,9,10 shows that the H-O-H bending vibration at about 1000 - 1600 cm^{-1}, typical of the H_2O molecule, is less intense. Thus, FTIR absorption spectroscopy allowed identifying the presence of certain types of chemical substances adsorbed on the surface of nanoparticles.

Resistance of the cell is affected by pH, volumetric concentration of ferrofluid, particle system used and inter-electrode spacing used. Present work aimed to fabricate usable network component for industrial applications at 300K. Various levels of static electric fields were applied to D1, D2 and D3 cells and it was observed that the resistivity decreases with increase in strength of static electric field in turn conductivity increases with increase in applied electric field. Volumetric concentration in present work was varied from 0.25% to 2%. Analysis for conductivity is given below.

Viscosity η is given by

$$\frac{\eta}{\eta_0} = 1 + 2.5\,\phi \qquad (2)$$

Dababneh et al have reported that ionic conductivity is dominant mechanism in ferrofluid which can be treated as dilute electrolyte system. Therefore charge on ions is given by

$$e = \pi\sqrt{\frac{\eta R_0 D^3}{\rho.f.\phi}} \quad \text{Columb} \qquad (3)$$

Lorentz force acting on ion is given by

$$F = e.\frac{V}{d} = \frac{\pi}{d}.V\sqrt{\frac{\eta R_0 D^3}{\rho.f.\phi}} \quad \text{Newton / ion} \qquad (4)$$

Hence energy per ion is given by,

$$-W = \int \left\{\frac{\pi}{d}.V\sqrt{\frac{\eta R_0 D^3}{\rho.f.\phi}}\right\} dl \quad \text{J/ion} \qquad (5)$$

Where,
V= potential difference between plates of the test cell.
d = inter-electrode separation
f = salt molecules were trapped in each Fe_3O_4 particle
ρ = resistivity,
η = viscosity of fluid
N = number of fine particles per unit volume,
R_0 = radius of salt molecule
D = Average diameter of nanoparticle
ϕ = volumetric concentration.

ISSN(Online) : 2319-8753
ISSN (Print) : 2347-6710

International Journal of Innovative Research in Science, Engineering and Technology

(An ISO 3297: 2007 Certified Organization)

Website: www.ijirset.com

Vol. 6, Issue 1, January 2017

Substituting Equation (2) in Equation (5) we have

$$-W = \int \left\{ \frac{\pi}{d} . V \sqrt{\frac{\eta_0 (1+2.5\phi) R_0 D^3}{\rho . f . \phi}} \right\} dl \qquad \text{J/ion} \qquad (6)$$

According to Equation (6), energy of ion is directly proportional to potential difference applied. Hence mobility of ion will increase for higher electric fields giving rise to higher conductivity and in turn lower resistivity. These results were verified from experimental observations and recorded in various tables given. That for constant static electric field, DC conductivity was found to increase with decreasing particle size because of total increased surface area with respect to particle volume. Hence, resistivity of ferrofluid decreases more for smaller particles prepared in pH 12 as compared to other particles prepared at pH8 and pH10. Further, it is observed for higher size particle system, total surface area with respect to particle volume decreases and hence ionic conduction is less predominant. The above observations were found consistent in D1, D2 and D3 test cells with variation in various volumetric fractions and various applied static electric fields which have been recorded in various tables. [21]

In subsequent experiments, higher differential variation in resistance was observed for different volumetric concentration (0.25%, 0.5%, 1% and 2%) for all the three particle systems and result was tabulated in Table 29, 30. These tables show the differential resistance with respect to differential potential from 0 Volts to 35 Volts. It is observed in table 29 that for cell D1, maximum differential resistance was found in lowest volumetric concentration(0.25%) and higher particle size(30nm).Similarly, for cell D1, minimum differential resistance was found in highest volumetric concentration (2%) and smaller particle size (10nm).Similar observations were found in D2 as well as D3 test cells.

Therefore, system having higher volumetric concentration and smaller particle size is suitable for making fix value resistor with certain tolerances. Similarly system having lower volumetric concentration and higher particle size is suitable for making Voltage Dependent Resistor (VDR). Commercially available VRD components in the market are in the range of few Ohms and are used for low voltage range, whereas experimentally prepared VRD was in the range of Mega-Ohms which has additional advantage over commercially available VDR that, this can be used in very high voltage ranges.

Table no. 29 Maximum and Minimum differential resistance for Cell D1,D2,D3

Differential Resistance	D1	D2	D3
ΔR @ (0V to 35V)max	227.59MΩ	228.47MΩ	240.84MΩ
	pH8	pH8	pH8
	Vol .Concentration (ϕ) = 0.25%	Vol .Concentration (ϕ) = 0.25%	Vol .Concentration (ϕ) = 0.25%
ΔR @(0V to 35V)min	134.7MΩ	130.61MΩ	145.71MΩ
	pH12	pH12	pH12
	Vol .Concentration (ϕ) = 2%	Vol .Concentration (ϕ) = 2%	Vol .Concentration (ϕ) = 2%

Very high value fixed resistor as well as variable resistors were also fabricated and used as high potential sensing and current sensing devices. All these components could be used in electrical network at around room temperature. Therefore, all the measurements have been carried out at 300 K. In industry, use of value of resistance is widely used because of

ISSN(Online) : 2319-8753
ISSN (Print) : 2347-6710

International Journal of Innovative Research in Science, Engineering and Technology

(An ISO 3297: 2007 Certified Organization)

Website: www.ijirset.com

Vol. 6, Issue 1, January 2017

calculations involved in those applications. Therefore, instead of conductivity, directly resistance parameter was used wherever necessary when referred to device as a component.

Table no. 30 Maximum, Minimum differential resistance for volumetric concentration 0.25%, 0.5%, 1%, 2%.

Differential Resistance	0.25%	0.5%	1%	2%
ΔR @(0V to 35V)max	240.84MΩ	189.86MΩ	187.74MΩ	170.45 MΩ
	pH8	pH8	pH8	pH8
	Cell D3	Cell D3	Cell D3	Cell D3
ΔR @(0V to 35V)min	194.66MΩ	152.82MΩ	151.22MΩ	116.51MΩ
	pH12	pH12	pH12	pH12
	Cell D1	Cell D1	Cell D1	Cell D1

VII. CONCLUSIONS

After analysis of all tables and figures, following is concluded-

- For a particular concentration, as applied static electric field between the electrodes in ferrofluid increases, the DC conductivity increases.
- It is also inferred that under applied constant static electric field, conductivity increases with increase in volumetric concentration of ferrofluid.
- For a constant applied static electric field, DC conductivity was found to increase with decreasing particle size because of the total surface area with respect to particle volume was increased and ionic conduction was predominant. On account of larger size particle system, the total surface area with respect to particle volume was decreased and the ionic conduction was less predominant.
- Ferrofluid with particle system of 10 nm in size at 0.25%,0.5%,1% ,2% volumetric concentrations with 3mm, 6mm and 9mm inter-electrode spacing was in-sensitive to variation of strength of applied static electric field as far as change in resistance was concerned. This system of ferrofluid is suitable for fixed resistance/impedance components.
- Ferrofluid with particle system of 30 nm in size at 0.25%,0.5%,1% ,2% volumetric concentration with 3mm, 6mm and 9mm inter-electrode spacing was sensitive to variation of strength of applied static electric field as far as change in resistance was concerned. This system of ferrofluid is suitable for making Voltage Dependent Resistor (VDR) as an electrical network component used for protection of electrical systems against high voltage spikes/transients.
- Changes in dimensions of test cell have no effect on the physical trends shown in the various parameters.

VIII. ACKNOWLEDGEMENTS

One of the authors gratefully acknowledges Indian Chemical Institute, Mumbai, India and Instrumentation lab, Delphi Powers Pvt. Ltd., Pune, India for their help in instrumentation.

REFERENCES

1. Jun,Y.W.Lee,J.H.;Cheon,J "Chemical design of nanoparticles probe for high performance magnetic resonance imaging",Angew.Chem.Int.Ed.,47,pp.5122-5135, 2008
2. Sudimack,J.B.A, Lee,R.J "Targeted drug delivery via the folate receptor". Advanced .Drug Deliv.Rev.41, pp.147-162, 2000
3. Jordan,A., Scholz,R., Maier-hauff,K., Johannsen M., Wust,P., Nadobny J, Schirra,H, Schmidt,H.;Deger,S.,Loening,S.et.al "Presentation of a new magnetic fluid hyperthermia". J.Magn.Magn.Mater, 22, pp 5118-5126, 2001.

ISSN(Online) : 2319-8753
ISSN (Print) : 2347-6710

International Journal of Innovative Research in Science, Engineering and Technology

(An ISO 3297: 2007 Certified Organization)

Website: www.ijirset.com

Vol. 6, Issue 1, January 2017

4. Hu,F.;Wei,L.; Zhou,Z.;Ran,Y.;,Z.; "Gao,M.Prepration of biocompatible magnetite nanocrystals for in vivo magnetic resonance detection of cancer", Adv.Mater",18,pp.2553-2556, 2006
5. V.A. Bambole, S. D. Kemkar, H. S. Mahajan, S. K. Gupta, "Electronic devices based on non linear characteristics of electron beam irradiated HPMC + PPy blends, National conference on advanced materials and technologies (NCAMDT-2008)", Sri Venkateshwara University, pp49-50. Feb 20-22, 2008
6. V.A.Bambole, H.S.Mahajan, S.K.Gupta, S.P.Koiry, S.D.Kemkar, "Study of variation of conductivity of electron beam irradiated HPMC+ PPy films with dose rate, National conference on advanced materials and technologies (NCAMDT-2008)",Sri Venkateshwara University pp. 161. Feb 20-22, 2008.
7. S.D.Kemkar, Sensor-13, "13th National Seminar, 2D Fractional microcontroller based tilt measurement system using ferrofluid", C-8-1, pp-32,March 3-5 2008.
8. S.D.Kemkar,"Design and Development of tilt angle measurement based on microcontroller system using ferrofluid", 52nd- DAE Solid State physics Symposium, Maysore,2007
9. S.D.Kemkar, H.S.Mahajan, M. Vaidya, "Ferrofluid based optical fiber switch, AIP Conference Proceedings", Vol 1447, pp.512- 522,2012.
10. S.D.Kemkar, H.S.Mahajan, Milind Vaidya, "Selective Switching action in optical fiber using fe_3O_4 based ferrofluid". Proceedings of International Conference in advances in computer and communication technology- ACCT, pp.14-15. 2012.
11. R.E.Rosensweig, Y.Hirota, S.Tsuda and K.Raj. "Study of audio speaker containing ferrofluid", J.Phys: Condens, Matter 20, 204147,pp-5. 2008.
12. S.Engelmann, A.Nethe, T.H.Scholz, H.D.Stahlmann, "Force enhancement on a ferrofluid-driven linear stepping motor model", JMMM pp. 272-276, 2345-2347, 2004.
13. G.Morton, W G Fruh, "The force on a object passing through a magnetic fluid seal", JMMM, 252, pp.324-326, 2002.
14. G.Schintie, P.Palade, L.Vekas, N.Iacob, C.Bartha, V.Kuncser, "Volue fraction dependant magnetic behavior of ferrofluids for rotating seal applications", J Phys. D Appl. Phys. 46, 395501 (8pp), 2013
15. R.P. Pant, S.K. Dhawan, N.D. Kataria, D.K. Suri, "Investigation on ferrofluid-conducting polymer composite and its application", JMMM 252, pp.16-19,2002
16. J Popelewell, P Davies, J.P. Llewellyn, K. O'grady, "Microwave properties of ferrofluid composites", JMMM 54-57 () 761-762, 1986
17. F. Pelegrini, A.R. Pereira, P.C. Morais, "Ferromagnetic resonance line of ferrite ferrofluid at high microwave power", JMMM 289 pp. 84-86, 2005.
18. V. A. Bambole, S. D. Kemkar , H . S. Mahajan, S. K. Gupta, "Electronic device based on nonlinear characteristics of electron beam irradiated hpmc + ppy blends, , National conference on advanced materials and technologies (NCAMDT-2008)", Sri Venkateshwara University. Feb 20-22, 2008
19. V.A.Bambole , H.S.Mahajan , S. K.Gupta, S.P.Koiry , S.D.Kemkar, "Study of variation of conductivity of electron beam irradiated hpmc + ppy films with dose rate, National conference on advanced materials and technologies (NCAMDT-2008)", Sri Venkateshwara University, Feb 20-22, 2008.
20. A.Javier, Lopez, Ferney González, A. Flavio, Bonilla, Gustavo Zambrano1, E. Maria, Gómez, "Synthesis and characterization of Fe_3O_4 magnetic nanofluid, Revista Latinoamericana de Metalurgia y Materials"; 30 (1):pp. 60-66, 2010.
21. M.S. Dababneh, N.Y.Ayoub, I.Odeh, N.M.Laham, "Viscosity,resistivity and surface tension measurements of Fe_3O_4 ferrofluid, J Magnetism Magnetic Material 125 pp.34-38,1993.